Passive Noise Suppression Methods for Improvement of Photoacoustic and Photothermal Measurements of Aerosol Light Absorption from Mobile Platforms

Control # 94

W. Patrick Arnott[1], Arthur J. Sedlacek[2], and John M. Hubbe[3]

[1]Dept of Physics and Atmospheric Science, University of Nevada Reno, Reno NV, 89557

[2]Brookhaven National Laboratory, Environmental Sciences Department, Upton, NY 11973-5000

[3]Pacific Northwest National Laboratory, ARM Aerial Facility, Richland, WA 99352

Introduction

Photoacoustic aerosol instruments employ a sensitive microphone to detect the often-low sound pressure levels produced when light absorbing aerosol are illuminated by modulated laser light. Photothermal instruments utilize an optical interferometer to detect air density fluctuations attendant to laser heating of air by light absorbing particles in its volume. Measurements are desired for fixed sites as well as for ground-based and aircraft mobile platforms that can spatially sample air pollution in a city or region downwind of sources such as forest fires. Of all the noise sources that must be dealt with for high quality measurements, the most challenging one is associated with extreme pressure fluctuations of the sample inlet system, especially for aircraft-based measurements when the plane is in the turbulent planetary boundary layer. This paper presents a summary of methods developed to suppress inlet noise. One technique is to employ an 'acoustic reflector, that is a simple short section of capillary tube. A ready implementation of the acoustic resistor is commercially available as a wire welding tip of diameter 0.025" and length 1". The second implement is a muffler constructed in a way to minimize particle loss while still attenuating sound. A few examples of measurements aboard the Department of Energy's Gulfstream-1 (G1) aircraft in summer 2013 during the Biomass Burning Observational Period campaign, before and after use of noise suppression are used below to illustrate the sound suppression effectiveness.

Aerosol light scattering and absorption measurements are used to quantify radiative forcing by particulate matter, with applications to climate and health (Bond, Doherty et al. 2013). Aerosol light absorption measurements by in situ methods are preferred over filter-based methods because they are more accurate (Sheridan, Arnott et al. 2005), though the latter has excellent precision (Springston 2007). Measurement precision is especially an issue when measuring from meteorological aircraft because of the turbulent environment and rapid changes of ambient pressure, temperature, and relative humidity (Sheridan, Arnott). These effects and their influences on photoacoustic sampling from aircraft have been described (Arnott, Walker et al. 2006).

Description of Methods to Reduce Measurement Noise

Figure 1 illustrates the problem. The blue (red) curve is the aerosol light absorption (noise equivalent aerosol light absorption) measurement prior to (10 Mm^{-1}) and during flight (up to 1000 Mm^{-1}). The spikes prior-to-flight were from BC emissions by other aircraft. Post flight

noise measurements as the aircraft taxied to the hangar were lower than inflight, indicating that most of the noise is due to the rush of air to and past the inlet system.

Figure 1. First flight illustrating the need for noise suppression.

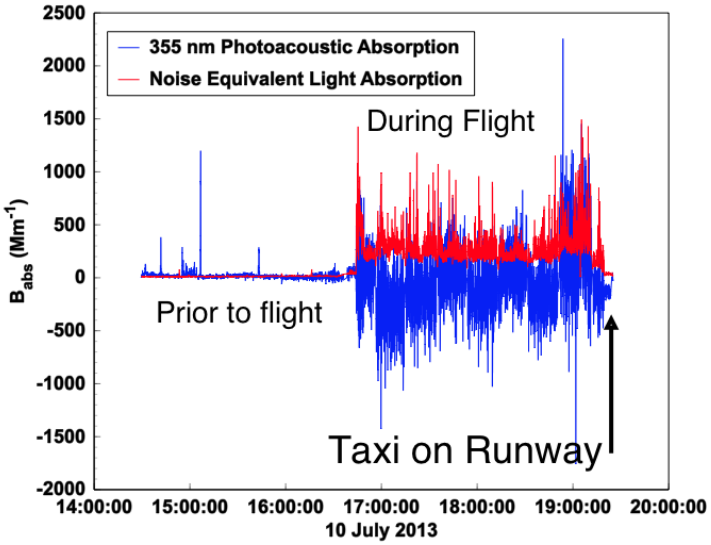

Figure 2. Sketch of the systems (muffler and acoustic reflector) used to reduce noise propagation from the aircraft inlet to the instrument.

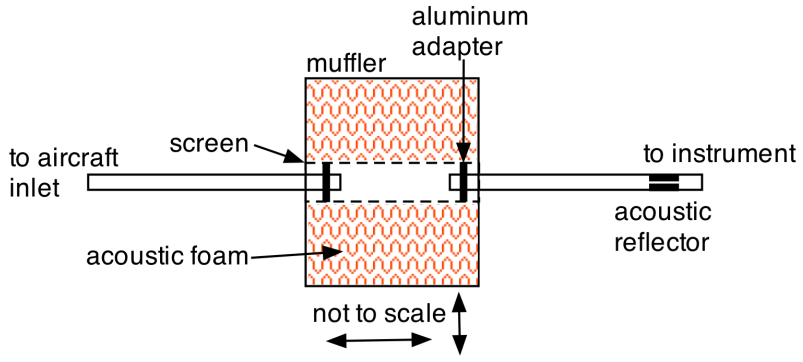

Figure 2 illustrates the muffler and acoustic reflector employed to reduce the effects of noise of the inlet system. The muffler dissipates sound by thermoviscous attenuation in the foam. The portion exposed to aerosol is metallic screen. Sound reflected by the acoustic reflector is returned to the muffler where it is dissipated further.

Figure 3 is the measured transfer function of the system showing a potentially large noise reduction potential (0 dB is no effect). The thick black curve is for both the muffler and reflector in Fig. 2. Figure 4 shows measurements in clear air obtained after the implementation of the noise reduction system, indicating a noise reduction by a factor of 10 compared with Fig. 1, and much more stable readings. Use of the instrument on the aircraft still causes noise to increase by a factor of 10 compared with lab use, likely as a result of the high sound pressure levels in the aircraft cabin. Structural vibration was mitigated with use of two aircraft tire inner tubes placed below and above the instrument.

Figure 3. Sound attenuation by both the muffler and acoustic reflector for the system shown schematically in Figure 3. Mufflers 1 and 2 had less acoustic foam.

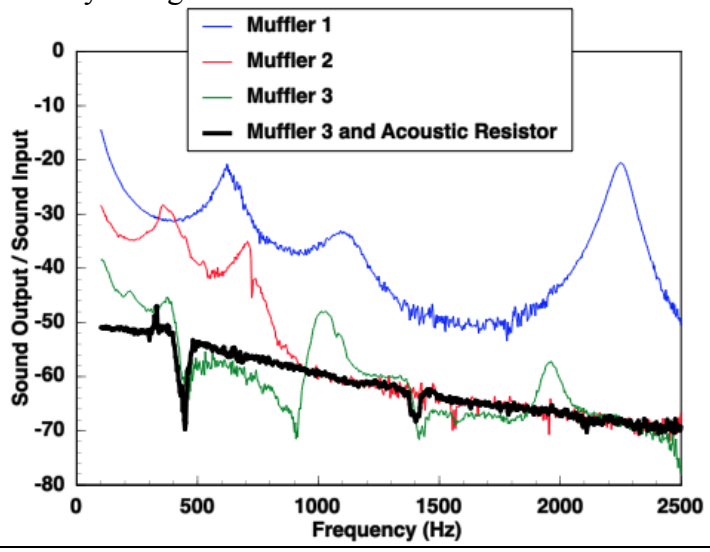

Figure 4. Clear air measurements aloft after installation of the noise reduction system. Top panel is light scattering at 355 nm, middle panel is light absorption and noise equivalent light absorption, and the bottom panel shows the resonator acoustics in flight.

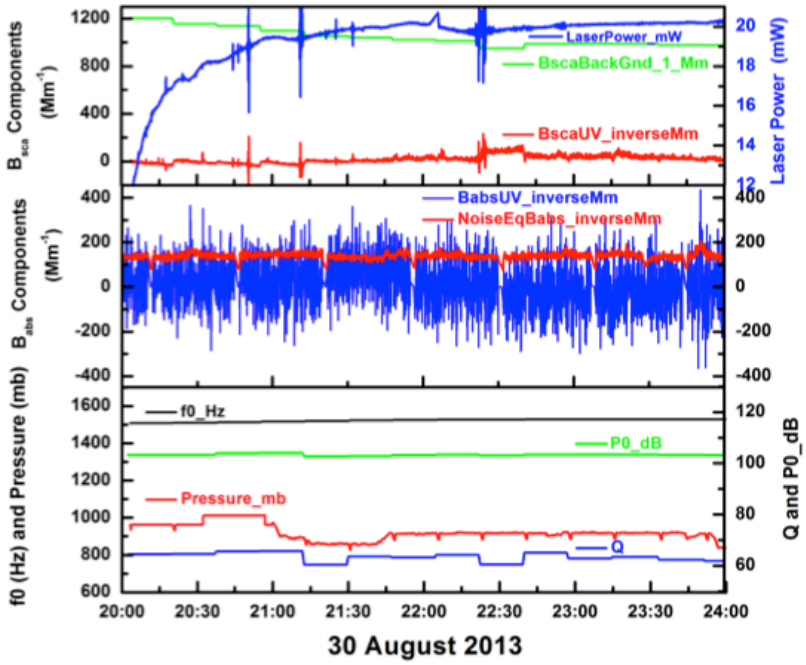

Details of the Acoustic Reflector

Figure 5 schematics the acoustic reflector and defines the variables for length and diameters. Assuming Poiseuille flow (that is, laminar flow with a strong influence of gas viscosity on making the flow profile in the core be parabolic shaped), the pressure drop across the reflector is given by

$$\Delta P = Q\frac{128\,\mu\,L}{\pi\,d^4} \quad , \tag{1}$$

where μ is the gas viscosity and Q is the volumetric flow rate. The average speed, v, of the flow in the acoustic reflector is

$$v = \frac{Q}{\pi d^2} = \frac{d^2\,\Delta P}{128\,\mu\,L} \quad . \tag{2}$$

The speed of sound, c, in the gas is the maximum speed. This condition for critical flow therefore is obtained for a pressure difference

$$\Delta P_{crit} = \frac{128\,c\mu\,L}{d^2} \quad . \tag{3}$$

It is desirable to keep the pressure gradient below the value given by Eq. 3 because the flow effectively carries sound through the interface under the condition of Eq. 3. Equations (1) through (3) express the low Reynolds number regime of direct flow through the orifice. The Reynolds number is about 2050 in the acoustic reflector, and is 223 in the conductive tubing that delivers sample air to the instrument.

Figure 5. Image (left) of the wire welding tips co-opted into service as acoustic reflectors. Schematic of the acoustic reflector is on the right. The outside diameter, D, matches the inside diameter of the conductive tubing used to convey sample air to the instrument.aircraft during the BBOP campaign. The orifice diameter d = 0.025".

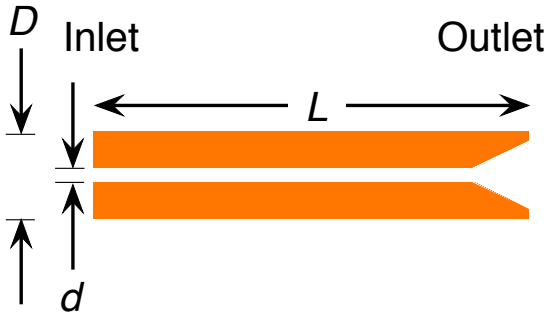

The small orifice depicted in Fig. 2 reflects sound coming in the inlet system. Figure 6 shows the arrangement used to quantify the amount of reflection as a function of the sound frequency. A hearing aid speaker and microphone were placed on the left end, and a second microphone on the right end. A long section of tube (not shown) was attached to the right end to approximate no reflection from the right end of the tube. The frequency dependent transfer function, $T(f)=mic2(f)/mic1(f)$, was measured and modeled to quantify the effectiveness of the reflector in reducing the output sound at *mic2*.

Figure 6. Sketch of method to measure transmission of sound through the acoustic reflector.

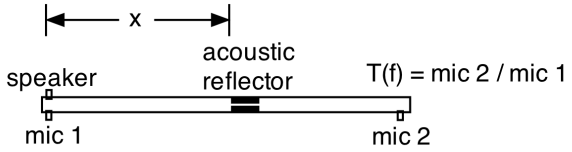

Measured and modeled transfer function results are shown in Fig. 7 along with the modeled properties of the characteristics of the sound propagation in the acoustic reflector. ***The resonance structure in the 15 cm measurements confirms that the mechanism of sound attenuation is reflection by the right side of the acoustic reflector due to a pressure release boundary condition.*** The resonance structure is caused by a standing wave that is set up between the acoustic reflector and *mic1*. The blue curves represent measurements and model for when the speaker and *mic1* are moved within 1 cm of the acoustic reflector. In this case the resonance structure is not visible because the frequency range of the measurement is too low. The short length pushes the resonance to higher frequency. The model is a complete linear solution of sound from the speaker to the microphones, as a numerical implementation of the theory in (Arnott 1991). Acoustic properties of the narrow tube in the reflector are shown on the right of Fig. 7. Shown are the phase speed relative to the adiabatic sound speed, attenuation, and characteristic impedance ratio for sound propagation through the acoustic reflector. The attenuation is less than -1.5 dB for the acoustic reflector, indicating that mechanism for sound reduction is not thermoviscous dissipation of sound in the short, narrow tube. The characteristic impedance ratio approaches unity above 100 Hz, indicating that the intuitive model for acoustic reflection by the open tube boundary condition at the right side of the acoustic reflector in Fig. 3 is viable.

Figure 7. Left. Model and measurement of sound attenuation through the acoustic reflector for the reference microphone x=1 cm and x=15 cm upwind of the acoustic reflector (see Fig. 6).

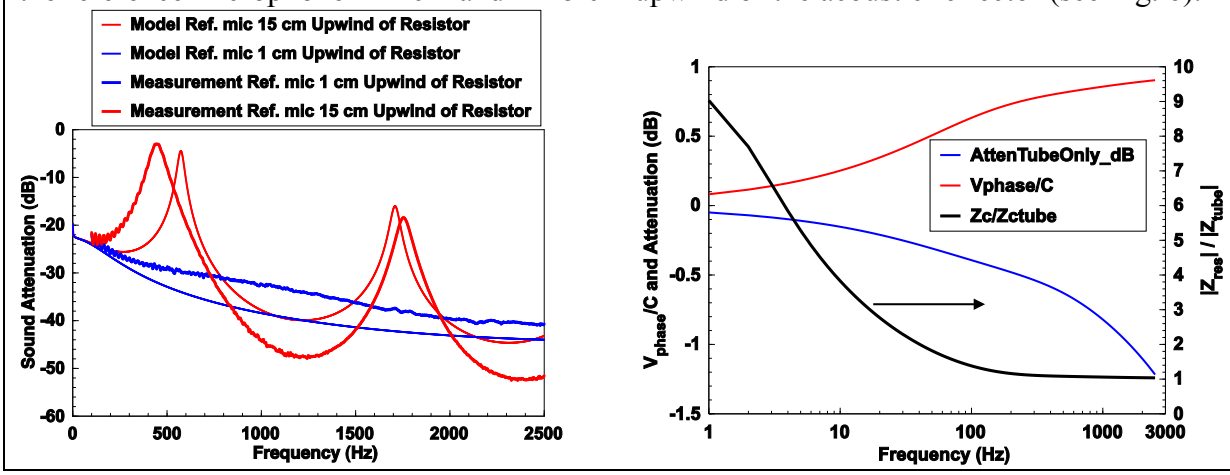

Details of the Muffler

Next we consider details of the muffler design. We needed to rapidly find a solution to the noise problem, so sought off the shelf components for the muffler, though it was also useful to make a few components in the machine shop. Figure 8 shows various images of the muffler design. A

roll of stainless steel screen is made (held circular by 4 metal cable ties). Acoustic foam is wound around the screen and both are placed inside the sewer pipe clean out T (the black case). The right image shows end cap. The aerosol path is fully enclosed by metal tubing and adaptor parts, and the 'dumbell' ensures contact with the metal screen. This way we were able to maintain a conductive path for the inlet system to minimize particle loss due to charge buildup. A healthy dose of teflon tape is used around the black end cap threads to seal the muffler.

While acoustic foam was used on the muffler interior, it would of course also be possible to fill this region instead with impregnated beads that could serve both the function of sound suppression as well as denuding certain chemical species such as NO_2 or water vapor that might cause measurement interference. The theory of sound propagation in porous material would guide design of bead size and/or morphology.

We chose to use passive sound suppression methods (muffler and reflector) rather than active methods like those employed with noise-cancelling headphones. Our choice was motivated by the need to have an immediate solution to our problem. It is likely that future efforts would benefit from a combination of active and passive noise cancelling techniques for sound suppression. For example, with the correct algorithm, the set up shown in Fig. 6 could be used to determine what sound needs to be delivered from the speaker to minimize sound passing through the right side of the system (past *mic2*).

Figure 8. Components of the muffler system.

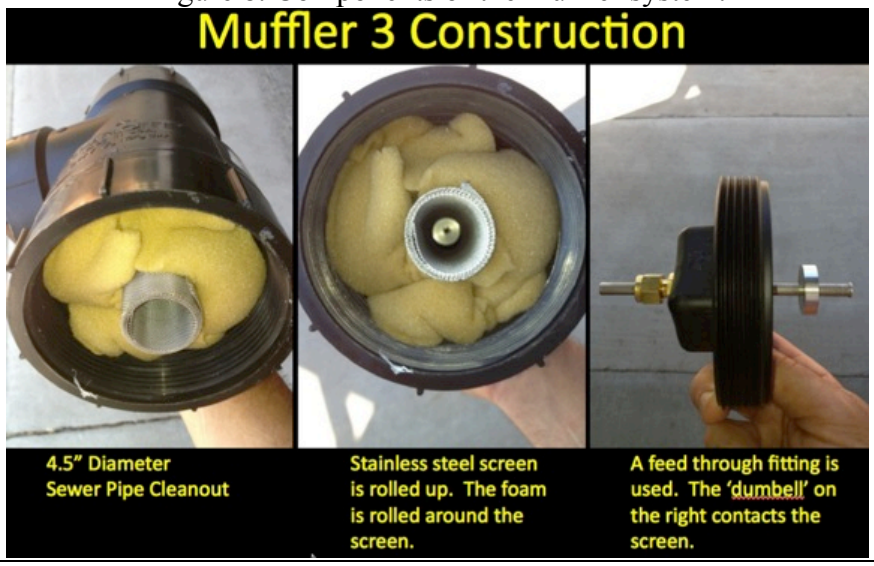

Our decision to use the photoacoustic instrument in this campaign was predicated upon having large signals caused by immense amounts of aerosol from wild land fires. The laser power we employed was only 20 mW, a factor of 10 to 50 lower than in most of our other aircraft campaigns. We were mostly interested in achieving measurements at 355 nm where little is known about the optical properties of aerosol.

Figure 9 shows an excellent measurement example taken from a fire sampled in Northern Oregon to illustrate the extremely high aerosol light absorption and scattering values one finds

very close to the source of the smoke. The single scattering albedo at 355 nm is 0.85. Acoustic noise is not an issue for these high concentrations, though noise suppression was helpful because we perform the instrument acoustic calibration about every 5 minutes during flight. Noise suppression greatly improves the acoustic noise calibration quality as well.

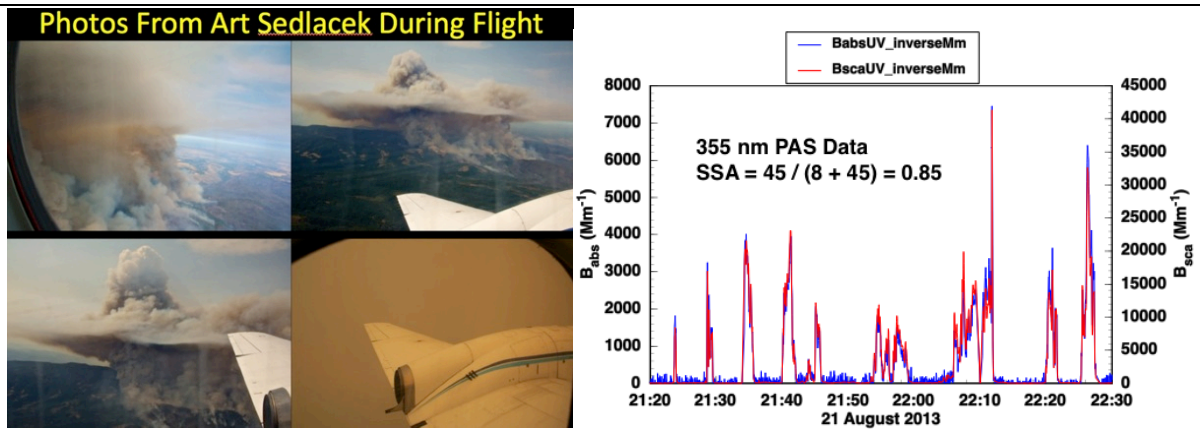

Figure 9. Left. Images of the Government Flats fire in Oregon on 21 August 2013. The DOE G1 aircraft penetrated the smoke close to the source of the fire. Right. Scattering and absorption by the smoke from the Government Flats fire in Oregon.

We acknowledge support from the Department of Energy for the field measurements reported here.

References

Arnott, W. P., Bass, Henry E., Raspet, R. (1991). "General formulation of thermoacoustics for stacks having arbitrarily shaped pore cross sections." Journal of the acoustical society of america **90**(6): 3228-3237.

Arnott, W. P., et al. (2006). "Photoacoustic Insight for Aerosol Light Absorption Aloft from Meteorological Aircraft and Comparison with Particle Soot Absorption Photometer Measurements: The DOE Southern Great Plains Climate Research Facility and the Coastal Stratocumulus Imposed Perturbation Experiments." Journal of Geophysical Research **111**(D05S02): doi:10.1029/2005JD005964.

Bond, T. C., et al. (2013). "Bounding the role of black carbon in the climate system: A scientific assessment." Journal of Geophysical Research: Atmospheres **118**(11): 5380-5552.

Sheridan, P. J., et al. (2005). "The Reno aerosol optics study: An Evaluation of Aerosol Absorption
Measurement Methods." Aerosol Science & Technology **39**: 1-16.

Springston, S. R., Sedlacek, A. J. (2007). "Noise characteristics of an instrumental particle absorbance technique." Aerosol Science and Technology **41**(12): 1110-1116.